Dalton Transactions

Oxidation of Uranium(IV) Mixed Imido-Amido Complexes with PhEEPh to Generate Uranium(VI) Bis(Imido) Dichalcogenolates, $U(NR)_2(EPh)_2(L)_2$

Journal:	*Dalton Transactions*
Manuscript ID	DT-ART-02-2019-000680.R1
Article Type:	Paper
Date Submitted by the Author:	13-Apr-2019
Complete List of Authors:	Tomson, Neil; University of Pennsylvania, Department of Chemistry Anderson, Nickolas; Los Alamos National Laboratory, Materials Physics and Applications Tontreau, Aaron; Los Alamos Natl. Lab, Chemistry Division Scott, Brian; Los Alamos National Laboratory, Materials Physics and Applications Boncella, James; Los Alamos Natl. Lab, Chemistry Division

Journal Name

ARTICLE

Oxidation of Uranium(IV) Mixed Imido-Amido Complexes with PhEEPh and to Generate Uranium(VI) Bis(Imido) Dichalcogenolates, $U(NR)_2(EPh)_2(L)_2$

Received 00th January 20xx,
Accepted 00th January 20xx

DOI: 10.1039/x0xx00000x

www.rsc.org/

Neil C. Tomson,† Nickolas H. Anderson, Aaron M. Tondreau, Brian L. Scott, and James M. Boncella*

This work provides new routes for the conversion of U(IV) into U(VI) *bis*(imido) complexes and offers new information on the manner in which the U(VI) compounds form. Many compounds from the series described by the general formula $U(NR)_2(EPh)_2(L)_2$ (R = 2,6-diisopropylphenyl, *tert*-butyl; E = S, Se, Te; L = py, EPh) were synthesized via oxidation of an *in situ* generated U(IV) amido-imido species with Ph_2E_2. This synthetic sequence provides a general route into *bis*(imido) U(VI) chalcogenolate complexes, circumventing the need to perform problematic salt metathesis reactions on U(VI) iodides. Investigation into the speciation of the U(IV) complexes that form prior to oxidation found a significant dependence on the identity of the ancillary ligands, with ^{t}Bu$_2$bpy forming the isolable imido-(bis)amido complex, $U(NDipp)(NHDipp)_2(^tBu_2bpy)_2$. Together, these data are consistent with the view that the *bis*(imido) U(VI) motif – much like the uranyl ion, UO_2^{2+} – is a thermodynamic sink into which simple ligand frameworks are unable to prevent uranium from falling when in the presence of a suitable retinue of imido proligands.

Introduction

Actinide chemists have made significant progress in the last decade at developing methods for generating multiple bonds between the 5f and p-block elements.[1-4] These efforts have dramatically expanded the scope of available actinide coordination compounds beyond the ubiquitous oxo ligand to include terminal chalcogenido, imido, and phosphinidene ligands on Th(IV),[5-10] U(IV-VI),[11-39] and Np(V).[40] The central drive behind this research has been to understand the factors governing the bonding in metals with diffuse and/or high-energy valence orbitals, especially the degree to which covalency may be invoked when describing interactions between actinide elements and their ligands.[41] The development of knowledge in this area contributes to fundamental advances in theoretical models, coordination chemistry, and catalysis as well as to separations technologies that are central to nuclear fuel reprocessing.

As an isoelectronic and isolobal analog to the uranyl ion (UO_2^{2+}), the *trans*-*bis*(imido) framework has provided a platform for studying the *trans*-E=U=E (E = O, NR) motif through modifications to the steric and electronic properties of the imido R group.[26, 27, 29] This work has provided a range of compounds that have contributed to the investigation of π-bonding to actinides. Variations in the R substituent include the use of alkyl and aryl groups of varying size, as well as aryl substituents with differing electron-donating/withdrawing abilities. These *trans*-*bis*(imido) compounds have been generated through three main pathways (Scheme 1), all of which involve oxidation of *in situ* generated uranium amine/amido/imido complexes.

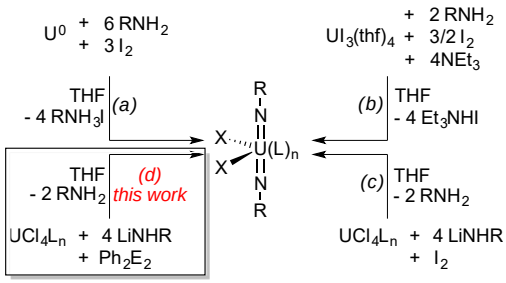

Scheme 1. Generalized routes for synthesizing $U^{VI}(NR)_2X_2L_n$ complexes from (*a*) uranium metal, (*b*) $UI_3(thf)_4$, (*c*) and (*d*) UCl_4.

In the original report of this motif, $U(N^tBu)_2I_2(thf)_2$ was synthesized through oxidation of U turnings by 3.0 equivalents of I_2 in the presence of 6.6 equivalents of ^{t}BuNH$_2$ (Scheme 1a).[29] Subsequent studies were able to show that $UI_3(thf)_4$[26] and UCl_4[12] were both suitable precursors for generating U(VI) *bis*(imido) complexes when treated with alkali metal amide salts, suggesting that the presence of ^{t}BuNH$_2$ was not necessary during the synthesis from metallic uranium until a mid-level oxidation state had been reached at the metal. It is unknown,

Chemistry Division, Los Alamos National Laboratory, MS J514, Los Alamos, New Mexico 87545, United States
Present Address. †P. Roy and Diana T. Vagelos Laboratories, Department of Chemistry, University of Pennsylvania, 231 South 34th Street, Philadelphia, Pennsylvania 19104, United States.

Electronic Supplementary Information (ESI) available: [details of any supplementary information available should be included here]. See DOI: 10.1039/x0xx00000x

however, what speciation the U(IV) amido precursors take prior to oxidation. For example, the treatment of UCl_4 with 4.0 equiv of LiNH^{t}Bu could yield, assuming complete substitution of the uranium chlorides, mononuclear complexes containing fragments ranging from $U(NH^tBu)_4$ to $U(N^tBu)(NH^tBu)_2$ to $U(N^tBu)_2$, the last of which would be of particular interest as a molecular analog to the networked solid framework of UO_2.

We recently reported that the treatment of $U^{IV}Cl_4(R_2bpy)_2$ (R = Me, ^{t}Bu) with 4.0 equiv of LiNHDipp (Dipp = 2,6-^{i}Pr$_2$-C$_6$H$_3$) gave the U(V) complex $U^V(NDipp)_2Cl(R_2bpy)_2$,[18] with the source of oxidation linked to the presence of adventitious CH_2Cl_2 (Scheme 2). Further work indicated that $U^{VI}(NAr)_2I_2(R_2bpy)$ (Ar = Dipp, Mes) could be generated from $U^{IV}Cl_4(R_2bpy)_2$ (R = Me, ^{t}Bu) upon treatment with 4.0 equiv of LiNHAr followed by 1.0 equiv of I_2 (Scheme 1c).[12] Taken together, these reactions suggest that an intermediate U(IV) compound with amido and/or imido ligands is present, but the speciation of the U(IV) complex formed prior to oxidation, as well as the potential for using various lower valent uranium amido/imido complexes as synthons for higher valent *bis*(imido) complexes remains undetermined.

Scheme 2.

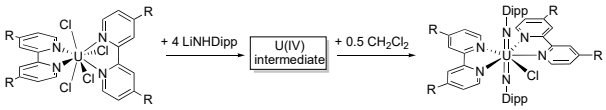

The present contribution seeks to provide insight into these problems by describing the syntheses of U(VI) *bis*(imido) compounds that proceed through U(IV) precursors, then investigating the nature of a U(IV) precursor to the U(V) and U(VI) species described above. Together, this work suggests that the exact speciation of low-valent amido/imido complexes may be irrelevant to the formation of U(VI) *bis*(imido) compounds, provided a suitable oxidant is present.

Results and Discussion

Synthesis of U(VI)-bis(imido) complexes.

The addition of 4.0 equiv of LiNHDipp to a THF solution of UCl_4 causes an immediate color change from green to dark red. After stirring for 5 min, the addition of Ph_2E_2 (E = S, Se) causes the color of the solution to lighten slightly. A diamagnetic product (**A**) is obtained by removing the volatile materials and extracting with Et_2O (Scheme 3). Attempts to isolate **A** in a crystalline form were unsuccessful due to the presence of excess NH_2DIPP, however compound's ^{1}H NMR spectroscopic data is remarkably similar to that of $U(NDIPP)_2(EPh)_2(thf)_2$ (E = S, Se),[42] with slight shifts due to the excess NH_2DIPP. Previous work in this area has encountered similar difficulty in purifying analogous U(VI) amine complexes.[26] While unambiguous analytical data are not currently available on **A**, we found that this material provided a convenient entry into a range of U(VI) *bis*(imido) complexes.

The addition of excess pyridine to **A** results in a color change and precipitation of the mononuclear complexes $U(NDipp)_2(EPh)_2py_2$ (E = S (**1-S**), Se (**1-Se**)) in good yields (**1-S**: 78%, **1-Se**: 85%)(Scheme 3). A crystal structure was obtained for the selenium complex (Figure 1), revealing molecular inversion symmetry, with the two pyridine and SePh ligands in a *trans* configuration. The steric imposition of the Dipp-^{i}Pr groups likely enforces the coplanarity of the pyridine rings with the plane of the equatorial ligands about the uranium center (C_{py}–N_{py} –U–Se torsion angle = 2.8°). For **1-Se,** as well as analogous structures described below, the crystallographic data are unexceptional, exhibiting U=NDipp bond distances of *ca.* 1.89 Å and U–EPh bond lengths consistent with those reported previously.[20]

Scheme 3.

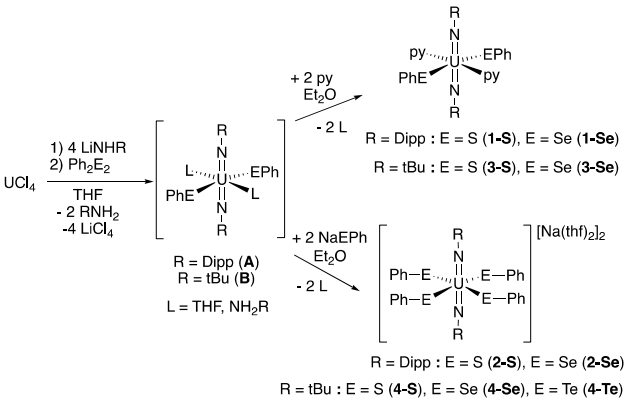

In lieu of neutral bases, the introduction of two equivalents of NaEPh•0.5thf to Et_2O solutions of **A** similarly results in the precipitation of microcrystalline solids and the formation of the "-ate" complexes $[Na(thf)_2]_2[U(NDipp)_2(EPh)_4]$ (E = S (**2-S**), Se(**2-Se**)) in good yields (**2-S**: 81%, **2-Se: 91%**) (Scheme 3). These species exhibit 4/mmm symmetry in solution, as observed by ^{1}H NMR spectroscopy, with a single set of resonances for both the Dipp groups and the Ph rings of the chalcogenolate ligands. The molecular structure of **2-S** (Figure 2) was found to include lithium counterions rather than sodium. Considering the high yield of **2-S**, the mass of salt collected when filtering ethereal solutions of **A** is too great for the lithium complex (**2-SLi**) to represent the majority of the isolated material.

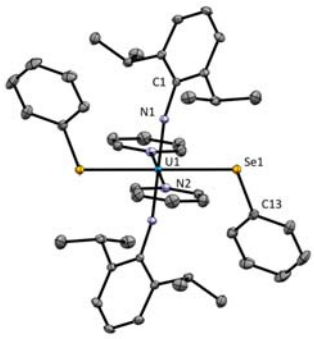

Figure 1. Molecular structure of **1-Se**, $U(NDipp)_2(SePh)_2py_2$; with atoms displayed as thermal ellipsoids at 50 % probability and hydrogen atoms removed for clarity. Bond distances (Å) and angles (°): U1–N1 1.8861(11), U1-N2 2.5926(12), U1-Se1 2.8299(2), U1-N1-C1 164.63(9), U1-Se1-C13 110.75(4).

Notably, we observe two crystal forms in the isolated material: a small amount of larger, high-quality crystals (**2-SLi**, used for XRD) and a larger portion of small crystals (**2-S**). For analysis however it was found that pure samples of **2-S** and **2-Se** could be obtained simply by switching from LiNHDIPP to NaNHDIPP in the initial synthetic method, however the pure products were found to be far less crystalline than the crude product.

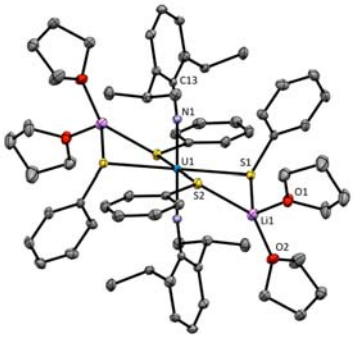

Figure 2. Molecular structure of **2-SLi**, $[Li(thf)_2]_2[U(NDipp)_2(SPh)_4]$: with atoms displayed as thermal ellipsoids at 50 % probability and hydrogen atoms removed for clarity. Bond distances (Å) and angles (°); **2-SLi**: U1–N1 1.8809(12), U1-S1 2.7434(4), U1-S2 2.8232(4), U1-N1-C13 173.38(10).

The crystal structure of **2-SLi** reveals a complex in which both Li ions are encapsulated within the secondary coordination sphere of the metal, forming a bridge between two adjacent SPh sulfur atoms. The distorted tetrahedral coordination sphere of Li is completed with two molecules of THF. To accommodate the steric imposition of the Dipp ^{i}Pr groups, the Ph ring of one pair of SPh rings is rotated into the S_4U plane: N1–U1–S2–C torsion angle = 97.6°; U1–S2–C–C torsion angle = 4.5°. This can be compared with the other set of symmetry related SPh ligands, which are nearly perpendicular to the S_4U plane (N1–U1–S2–C torsion angle = 9.9°) and rotate to accommodate the requirements of the Dipp arene (U1–S2–C–C torsion angle = 37.9°).

By substituting $LiNH^tBu$ for LiNHDipp, the identical reaction sequence described above can be used to generate the analogous complexes of the form $U(N^tBu)_2(EPh)_2L_2$. The addition of 4.0 equiv. of $LiNH^tBu$ to a THF solution of UCl_4 results in an immediate color change from green to dark orange. The subsequent addition of Ph_2E_2 (E = S, Se, Te) causes the solutions to change from dark orange to cherry red. Removal of the volatile materials under vacuum yields an oily residue, from which the U-containing products may be extracted into Et_2O to separate LiCl.

Solutions of this diamagnetic complex, presumed to be $U(NtBu)_2(EPh)_2(thf)_2$ (**B**, Scheme 3) proved to be suitable starting points for generating adducts of $[U(L)_2(N^tBu)_2(EPh)_2]$. Analogous to the procedure for synthesizing **2-E**, the addition of pyridine to solutions of **B** results ligation of the pyridine and the formation of $U(N^tBu)_2(EPh)_2(py)_2$ (E = S (**3-S**), Se (**3-Se**), Te (**3-Te**)) in good yields (**3-S**: 86%, **3-Se**: 87%, **3-Te**: 91%) (Scheme 3). ^{1}H NMR spectra of these compounds reveal broadened signals for the pyridine ligands, which could be indicative of either labile coordination to the metal center or intramolecular rearrangement processes. However, a rearrangement process seems unlikely, considering the multiple π-bonds between the metal center and the *trans*-imido groups, leading us to favor ligand dissociation as the origin of the dynamic behavior on the NMR timescale. The py ligands could adopt either a *cis* or a *trans* orientation within the equatorial plane of the complex. Related work with mono-dentate Lewis bases (triphenylphosphine oxide) found the presence of both isomers in solution.[20] In the present case, only one isomer was observed, but the symmetry of the complex did not allow for the determination of which isomer was present using the NMR data alone.

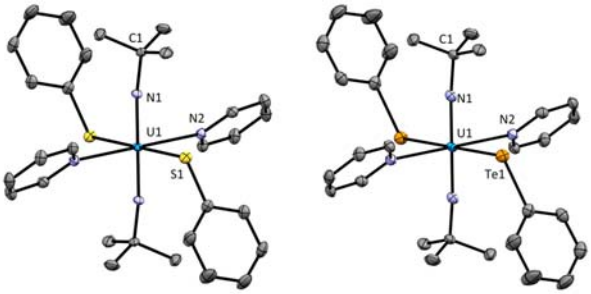

Figure 3. Molecular structure of **3-S**, $U(N^tBu)_2(SPh)_2(py)_2$ and **3-Te**, $U(N^tBu)_2(SPh)_2(py)_2$; with atoms displayed as thermal ellipsoids at 50 % probability and hydrogen atoms removed for clarity. Bond distances (Å) and angles (°); **3-S**: U1–N1 1.8617(16), U1-N2 2.5528(17), U1-S1 2.7297(5), U1-N1-C1 172.96(14). **3-Te**: U1–N1 1.858(3), U1-N2 2.562(3), U1-Te1 3.0544(3), U1-N1-C1 174.41(19).

The SPh complex **3-S** and the TePh complex **3-Te**, crystallized from ether to yield material of suitable quality for XRD (Figure 3). Refinement of the data revealed that both **3-S** and **3-Te** are centrosymmetric molecules that crystallized in the space group *P*-1. Structural characterization of U–Te bonds remains rare, with < 20 examples in the Cambridge Structural Database (CSD) and only two containing tellurolate ligands (RTe^-) coordinated to U(VI), both of which exhibit a terminal coordination mode. Of the two known examples of tellurolate ligands bridging two uranium centers, the U–Te distances are long, ranging from 3.119-3.372 Å.[43, 44] In both examples, the metal centers are in the +4 oxidation state. For **3-Te** we see a U-Te distance that is slightly shorter than these standards, with a bond distance of 3.0544(3) due to the decreased ionic radius of the U(VI) oxidation state.

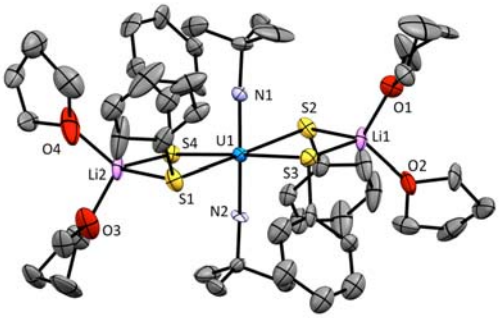

Figure 4. Molecular structure of **4-SLi**, $[Li(thf)_2]_2[U(N^tBu)_2(SPh)_4]$, with atoms displayed as thermal ellipsoids at 50 % probability and hydrogen atoms removed for clarity. Bond distances (Å) and angles (°); **4-SLi**: U1–N1 1.835(6), U1–N2 1.848(5), U1-S1 2.790(2), U1-S2 2.787(2), U1-S3 2.775(2), U1-S4 2.773(2), U1-N1-C1 174.3(5), U1-N2-C4 174.3(5).

When starting with solutions of **B**, the equatorially homoleptic dianions $[Na(thf)_2]_2[U(N^tBu)_2(EPh)_4]$ (E = S (**4-S**), Se (**4-Se**), Te (**4-Te**)) can also be synthesized in good yields and high purities by adding two equivalents of NaEPh•0.5 THF to the stirred ether solution of **B** (**4-S**: 72%, **4-Se**: 83%, **4-Te**: 93%) (Scheme 3). Within minutes, the products precipitate as microcrystalline solids, ranging in color from yellow (E = S) to orange (E = Se) to dark green (E = Te). The products were recrystallized from evaporating ether solutions, yielding XRD quality crystals in the cases of the Li salt of **4-S (4-SLi)** and **4-Te**.

The crystalline material obtained for **4-S** had the same characteristics of **2-S**, in that a small number of XRD-quality crystals were found among a large portion of crystallites. The collected XRD data again found a species in which Li – not Na – was included in the coordination sphere (Figure 5). The U–S bond lengths in **4-SLi** ranging from 2.790(2) and 2.773(2) Å are elongated from the neutral pyridine complex **3-S** (U–S = 2.730 Å). In an ion-paired "-ate" complex, one would typically assign this bond lengthening to a repulsive electrostatic effect, but the incorporation of Li in the coordination sphere (S–Li = 2.460-2.562(12) Å) could cause the U–S interaction to weaken due to the bridging character of the thiophenolate ligand. The structure of **4-S** is also notable for the canting of the S_4 plane with respect to the N–N vector. The *ca*. 10° distortion also occurs in the other tetra-chalcogenolato compounds (see below) and appears to be driven by steric interaction of the EPh aryl rings with the alkali metal-coordinated THF residues. Again, the phenyl rings are constrained to the vicinity of the ^{t}Bu groups, causing a downfield shift of the ^{t}Bu methyl groups in the ^{1}H NMR spectrum for all **4-E** complexes to *ca*. 0.2 ppm. Coordinated THF is not observed when spectra are recorded in THF-d_8, but NMR data collected in CD_2Cl_2 reveals signals for THF that are modestly shifted from those of free THF in solution.

The molecular structure of **4-Te** is shown in Figure 5. Each Na cation forms a bridge between two adjacent Te atoms, but the preference for higher coordination numbers at Na, along with the greater steric accessibility of Te, leads to a network chain involving butterfly-type dimerization through one of the Na-Te units. The sodium cation is pentacoordinate, forming a square-based pyramid (τ = 0.15) with one three-coordinate Te, two four-coordinate Te, and two molecules of THF. The three-coordinate Te exhibits significant pyramidalization (Σ(angles) = 302.3°), but the four-coordinate Te adopts a *cis*-divacant octahedral, or see-saw, geometry. It is interesting to compare the U–Te (3.099 Å) and Na–Te (3.230 Å) bond lengths, for which the U–Te distances are *ca*. 0.13 Å shorter and in agreement for what was seen with **3-Te**. The ionic radius of octahedral U(VI) has been estimated at 0.87 Å,[45] *ca*. 0.28 Å smaller than the 1.14-1.16 Å values of 4-6 coordinate Na(I), meaning that if we assume negligible covalent character in the Na–Te bond, then the U–Te bond may also be reasonably described as ionic in character. Recent experimental and computational studies on $Tp^*_2U(TePh)$ (Tp* = *tris*(3,5-dimethylpyrazolyl)hydridoborate) identified the U–Te interaction in this U(III) complex as largely ionic.[46]

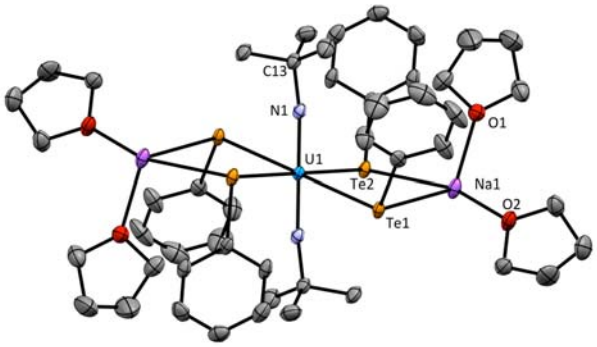

Figure 5. Molecular structure of **4-Te**, $[Na(thf)_2]_2[U(N^tBu)_2(TePh)_4]$, with atoms displayed as thermal ellipsoids at 50% probability. A single sub-unit of **4-Te** has been displayed and hydrogen atoms removed for clarity. Bond distances (Å) and angles (°); **4-Te**: U1–N1 1.855(4), U1-Te1 3.0990(4), U1-Te2 3.1175(4), U1-N1-C1 172.1(3).

The bipyridyl complexes $U(N^tBu)_2(EPh)_2(tBu_2bpy)$ (tBu_2bpy = 4,4'-ditertbutyl-2,2'-bipyridyl) can also be synthesized by the addition of a stoichiometric amount of tBu_2bpy to solutions of **B**, and they were found to be analytically identical to those reported previously.[20] Similarly, preliminary work has suggested that a range of Lewis bases can be used when generating compounds of the form $U(NR)_2(EPh)_2L_2$, but a full accounting of this work is beyond the scope of this manuscript. Instead, we will focus on the speciation of the U(IV) compounds that precede the U(VI) species described above.

Characterization of U(IV) imido/amido complexes.

Having recognized that these mixtures of UX_4 and M-NHR have proven successful starting materials for oxidation and the formation of both U(V) and U(VI) bis(imido) complexes by use of a number of different oxidants, including adventitious CH_2Cl_2,[18] the true nature of this mixture has remained reclusive. In order to accomplish this, the atmosphere of the glovebox was rigorously purged of all CH_2Cl_2 and related oxidants to prevent adventitious oxidation, which appears to be quite facile. Unfortunately, all attempts to isolate the products that result from treating UCl_4 with 4.0 equiv of LiNHR in THF have been unsuccessful, but analysis of crude solutions of the two by ^1H NMR provided useful insight into the nature of the reaction sequence that leads to U(VI).

The addition of 4.0 equiv of LiNHDipp to 1.0 equivalents of UCl_4 (precursor to **A**) in THF-d_8 generated a dark red/brown solution, and this crude mixture was analyzed by ^1H NMR spectroscopy. While analyzing the free diamagnetic material we see that approximately two equivalents of NH_2DIPP are released into the solution (as compared to the Cp_2Fe internal standard). This data would suggest that the identity of the U-based material in the crude mixture to be some derivative of $[U(NDipp)_2(thf)_x]_y$, (Scheme 4). However, due to the slightly broadened nature of the NH_2DIPP in solution, we believe that there may be some established equilibrium between that and $[U(NDipp)(NHDipp)_2(thf)_x]_y$. When moving to smaller NH_2R groups, as would be expected, this equilibrium is shifted further to the $[U(NR)(NHR)_2(thf)_x]_y$ side of the equilibrium. This is observed in the addition 4.0 equivalents of LiNHMes to 1.0 equivalent of UCl_4 resulting again in a red colored solution which was then analyzed by 1H NMR. Analysis of this solution by ^1H NMR spectroscopy revealed paramagnetic products along with only a single equivalent of free H_2NMes, suggesting that an imido/*bis*-amido product of the composition $[U(NMes)(NHMes)_2(thf)_x]_y$ was being generated in solution (Scheme 4).

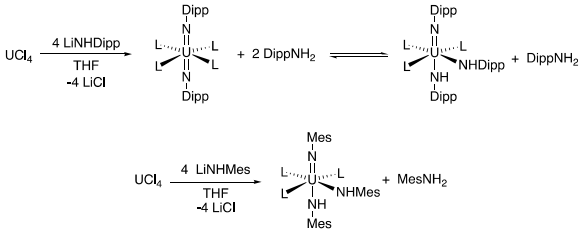

Scheme 4.

While attempts at isolating the putative $[U(NDipp)_2(thf)_x]_y$ product were unsuccessful in our hands, it was thought that by stabilizing the "$U(NDipp)_2$" unit with bulky ancillary ligands, the isolation of such a species might be possible. The addition of four equivalents of LiNHDipp to a stirred solution of $UCl_4(^tBu_2bpy)_2$ in THF resulted in an immediate color change from green to dark red. Crystallization from toluene/hexane produced a small quantity of black crystals, which display paramagnetically shifted NMR resonances.

An X-ray crystallographic study revealed a pseudo-pentagonal bipyramidal structure, with two $^tBu_2bpy$ ligands about the equatorial plane, along with three meridonally distributed NDipp-containing units (Figure 6). The $U\text{-}N_{Dipp}$ bond lengths were found to be U-N(1) = 2.095(7) Å, U-N(2) = 2.153(8) Å, and U-N(3) = 2.375(6) Å. These ligands exhibit obtuse U–N–C angles, ranging from 167.9(7)° for U-N(1)-C to 163.6(6)° for U-N(2)-C and 157.4(6)° for the U-N(3)-C angle of the equatorial ligand.

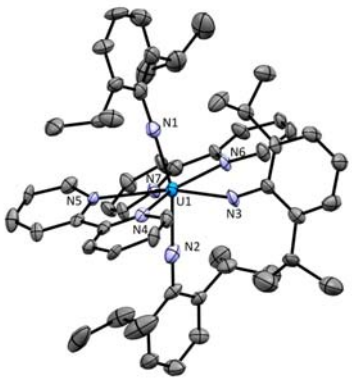

Figure 6. Molecular structure of **5**, $U(NDipp)(NHDipp)_2(^tBu_2bpy)_2$, with atoms displayed as thermal ellipsoids at 50 % probability and hydrogen atoms removed for clarity. Bond distances (Å) and angles (°); **5**: U1–N1 2.095(7), U1-N2 2.153(8), U1-N3 2.375(6), U1–N1-C1 167.9(7)°, U1-N2-C13 163.6(6)°, U-N(3)-C 157.4(6)°.

The unusual bond lengths and wide U–N–C angles hinder immediate identification of the product. However, given *i*) the paramagnetism of the complex, *ii*) the three NDipp-containing units, and *iii*) the overall neutral charge, four possible structures could be postulated (Figure 7): a U(III) *tris*-anilido, U(IV)

imido/*bis*-anilido, U(IV) *bis*-imido/aniline, and U(V) *bis*-imido/anilido (Figure 7, a – d respectively).

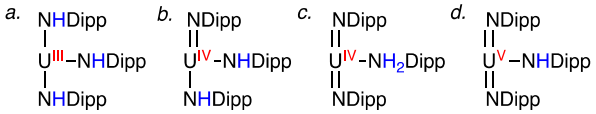

Figure 7. Oxidation state and protonation state possibilities for compound **5**.

The U–N(1) distance is short for an amido ligand on U(III). The shortest known primary amido bond to U is 2.156 Å for a U(IV) alkylamido complex.[47] Considering the larger ionic radius of U(III), the formalism of Figure 7a appears unlikely. Similarly, the U–N(1) and U–N(2) interactions are too long for a U(V) imido bond. The U=N bond lengths in the structurally related U(V) *bis*(imido) halides range from 1.942-1.980 Å, *ca.* 0.2 Å shorter than U–N(2); this excludes the formalism in figure 7d. Finally, the shortest known uranium bond to an amine ligand is in the recently reported U(VI) nitride, for which the U–NR_3 bond *trans* to the nitride has a U–N distance of 2.465 Å.[15] With a U–N(3) distance of 2.375 Å, the N(3)Dipp group is too short to the metal to be an amine ligand ruling out the structure in Figure 7c. Also considered was the redox non-innocence of the bpy ligand; however, with C(2)–C(2') distances of *ca*. 1.48 Å, this formulation can similarly be excluded.[48] The only remaining structural possibility is that of the U(IV) imido/*bis*-amido pictured in Figure 7b complex U(NDipp)(NHDipp)$_2$(^{t}Bu$_2$bpy)$_2$ (**5**, Scheme 5).

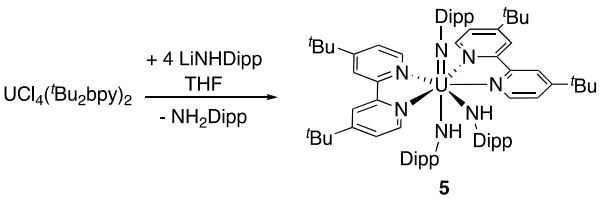

Scheme 5.

The longer than average U–N(1) imido bond distance of 2.100 Å is unusual and deserves comment. Bart and coworkers recently reported (^{Mes}PDI^{Me})U(NDipp)$_3$ (^{Mes}PDI^{Me} = 2,6-di(*N*-mesitylimino)pyridine),[14] featuring three NDipp groups in a T-shaped geometry about the metal center. The U=NDipp bonds of (^{Mes}PDI^{Me})U(NDipp)$_3$ lie between 1.99 Å (axial) and 2.03 Å (equatorial), considerably longer than those of U(Dipp)$_2$(I)$_2$(^{t}Bu$_2$bpy) at *ca*. 1.87 Å. Competition for π-bonding at the metal center was proposed to account for the dramatic increases in the U–N bond distances. A similar factor could be at work in **5**, as could steric effects from the congested heptacoordinate metal center with meridionally disposed NDipp-containing groups. Meyer and co-workers reported the longest known U=NR interaction (2.1219(18) Å) and attributed both the length of the bond and the reactivity of the imido functional group to steric pressure from the ligand framework.[28] U(IV) imido complexes with coordination spheres similar to that of **5** display U=NR bond lengths in the range of 1.99 Å.[12] Considering the 0.12-0.16 Å bond lengthening observed in both Bart's (^{Mes}PDI^{Me})U(NDipp)$_3$ and Meyer's ((^{Ad}ArO)$_3$tacn)U(NSiMe$_3$), we propose that steric pressure and a larger metal ionic radius could combine to account for the long U=NDipp bond in **5**. We also note that the imido/*bis*-amido formulation is consistent with the notion that the polarity of a U(IV) imido bond would make the N atom more basic than that of either a U(V) or U(VI) imido. While mononuclear U(V) and U(VI) *trans-bis*(imido) complexes are known, the N atoms in an analogous U(IV) *trans-bis*(imido) species may be too basic in the presence of an aniline to be stable with respect to deprotonation of aniline. This idea is consistent with the behavior of the UO_2 fragment, which is readily isolable as the uranyl ion UO_2^{2+} and is known as UO_2^{1+}, but molecular UO_2 exists as a networked solid, highlighting the increased basicity of the lower valent uranium-oxygen multiple bond.

These findings reinforce the notion that, like its uranyl counterpart, the U(VI) *bis*(imido) moiety functions as a thermodynamic sink, wherein the exact coordination environment and protonation state of lower valent starting materials is unimportant to the outcome of oxidation reactions, provided a suitable pathway exists to oxidize the metal and remove excess protons on the imido pro-ligands. Should this be the case, then hydrogen atom abstraction from amido groups bound to a low valent uranium center may similarly produce a U(VI) *bis*(imido) framework. In this scenario, loss of H• from a primary amido ligand would simultaneously oxidize the metal and populate a U–N π-bonding orbital. This reaction is known in transition metal chemistry[49-52] but has not previously been applied to the f-block elements, and represents a future direction of this work.

Experimental

General. All reactions and subsequent manipulations were performed under anaerobic and anhydrous conditions either under high vacuum or an atmosphere of argon. Hexane, THF, diethyl ether, and toluene were purchased as anhydrous solvents and stored over activated 4Å molecular sieves for 24 h before use, then degassed through repeated exposure to a vacuum until the solvent bottle became cool to the touch. All NMR solvents were dried over activated 4Å molecular sieves prior to use. UCl_4,[53] and LiNH(2,6-^{i}Pr$_2$C$_6$H$_3$)[54] were synthesized by the published procedures. All other reagents were purchased from commercial suppliers and used as received. NMR experiments were performed on a Bruker Ascend 400 NMR spectrometer. NMR spectra are referenced to external $SiMe_4$ using the solvent peaks as internal standards. Elemental analyses were performed at Atlantic Microlabs.

U(NDipp)$_2$(EPh)$_2$py$_2$ (E = S (1-S), Se (1-Se)) and [Na(thf)$_2$]$_2$[U(NDipp)$_2$(EPh)$_4$] (E = S (2-S), Se (2-Se)). UCl_4 (150 mg, 0.4 mmol, 1 equiv) was dissolved in THF forming a green solution. LiNHDipp (289 mg, 1.2 mmol, 4 equiv) was added as a solid, causing the color of the solution to rapidly turn dark red. After stirring for 30 min at ambient temperature, PhEEPh (0.4

mmol, 1 equiv) was added as a solid. The color of the solution lightened slightly to a cherry red. This solution was stirred for 2 h, and then the volatile materials were removed under vacuum to give a tacky, oily residue. Dissolution in Et_2O (ca. 5 mL) yielded a red solution with a pale brown precipitate. Filtration through a plug of Celite provided a clear red solution (**A**), to which was added the desired Lewis base (2 equiv. py, or 2 equiv. NaEPh•0.5thf). The solution containing pyridine was allowed to stand at room temperature, yielding black crystals of $U(NDipp)_2(EPh)_2py_2$. Stirring the mixtures containing NaSPh•0.5thf resulted in rapid dissolution of the base, with concomitant deposition of the products as microcrystalline solids. After stirring for 30 min, the products were collected by filtration. **$U(NDipp)_2(SPh)_2(py)_2$ (1-S)**: ^{1}H NMR (C_6D_6, 293 K): δ 0.76 (d, 24 H, CH*Me*$_2$), 3.96 (sept, 4H, C*H*Me$_2$), 5.70 (t, 2H, Dipp *p*-H), 6.60 (t, 2H, py/SPh *p*-H), 6.87 (m, 6H, py/SPh *p*-H + py/SPh *m*-H), 6.98 (d, 4H, Dipp *m*-H or SPh *o*-H), 7.04 (t, 4H, py/SPh *m*-H), 7.83 (d, 4H, Dipp *m*-H or SPh *o*-H), 10.84 (m, 4H, py *o*-H) ppm. $^{13}C^{36}$ NMR (C_6D_6, 293 K): δ 24.96, 26.49, 118.54, 124.40, 125.18, 134.33, 138.22, 145.60, 150.04, 152.57 ppm. Analysis: Calc. (C, 57.18; H, 5.64; N, 5.81) Found. (C, 56.58; H, 5.39; N, 6.39) **$U(NDipp)_2(SePh)_2(py)_2$ (1-Se)**: ^{1}H NMR (C_6D_6, 293 K): δ 0.77 (d, 24 H, CH*Me*$_2$), 4.04 (sept, 4H, C*H*Me$_2$), 5.70 (t, 2H, Dipp *p*-H), 6.63 (t, 2H, py/SePh *p*-H), 6.87 (m, 6H, py/SePh *p*-H + py/SePh *m*-H), 6.93 (t, 4H, py/SePh *m*-H), 7.01 (d, 4H, Dipp *m*-H or SePh *o*-H), 7.94 (d, 4H, Dipp *m*-H or SePh *o*-H), 10.86 (m, 4H, py *o*-H) ppm. $^{13}C\{^1H\}$ NMR (C_6D_6, 293 K): δ 25.43, 27.06, 118.97, 125.33, 127.93, 128.20, 128.53, 135.36, 138.28, 138.73, 150.92, 152.80, 155.95 ppm. Analysis Calc (C, 48.01; H, 4.92; N, 3.11) Found (46.72; H, 5.23; N, 3.74) **$[Na(thf)_2]_2[U(NDipp)_2(SPh)_4]$ (2-S)**: ^{1}H NMR (C_6D_6, 293 K): δ 1.34 (br s, 16 H, THF), 1.52 (d, 24 H, CH*Me*$_2$), 3.49 (br s, 16 H, THF), 5.12 (sept, 4H, C*H*Me$_2$), 5.97 (t, 2H, Dipp *p*-H), 7.10 (t, 4H, SPh *p*-H), 7.35 (d, 4H, Dipp *m*-H), 7.44 (t, 8H, SPh *m*-H), 8.58 (d, 8H, SPh *o*-H) ppm. $^{13}C\{^1H\}$ NMR (C_6D_6, 293 K): δ 24.94, 26.53, 68.01, 118.78, 123.76, 126.79, 135.07, 145.66, 151.31, 154.98. Analysis: Calc. (C, 53.82; H, 5.08; N, 2.62) Found (C, 54.10; H, 5.44; N, 2.26) **$[Na(thf)_2]_2[U(NDipp)_2(SePh)_4]$ (2-Se):** ^{1}H NMR (C_6D_6, 293 K): δ 1.09 (br s, 16 H, THF), 1.30 (d, 24 H, CH*Me*$_2$), 3.19 (br s, 16 H, THF), 4.94 (sept, 4H, C*H*Me$_2$), 5.66 (t, 2H, Dipp *p*-H), 6.76 (t, 4H, SePh *p*-H), 7.00 (t, 8H, SePh *m*-H), 7.10 (d, 4H, Dipp *m*-H), 8.33 (d, 8H, SePh *o*-H) ppm. $^{13}C\{^1H\}$ NMR (C_6D_6, 293 K): δ 24.94, 27.04, 68.02, 118.77, 124.58, 127.02, 135.83, 138.00, 152.00, 155.64. Analysis Calc. (C, 49.68; H, 5.60; N, 1.81) Found (C, 49.50; H, 5.67; N, 1.92)

$U(N^tBu)_2(EPh)_2L_2$ (E = S, Se, Te; L = py) and $[Na(thf)_2]_2[U(N^tBu)_2(EPh)_4]$. To a pale-green solution of UCl_4 (200 mg, 0.52 mmol, 1 equiv) in THF (5 mL) at room temperature was added solid LiN^tBu (166 mg, 2.10 mmol, 4 equiv) in one portion. The color immediately turned orange, and the solution was stirred at ambient temperature for 30 min. PhEEPh (0.52 mmol, 1 equiv) was then added to the reaction mixture as a solution in THF, which resulted in an immediate color change to red. After stirring for 2 h, the volatile materials were removed under vacuum, and the residue was extracted with 5 mL Et_2O. The solution was filtered through Celite to remove a white solid and generate a clear red filtrate (**B**). Addition of either 2 equivalents of pyridine or NaEPh•0.5thf (8 mmol, 2 equiv) resulted in precipitation of the product as a microcrystalline solid, which was isolated by filtration and crystallized using a hexane diffusion into toluene (**3**) or slow evaporation of a 4:1 Et_2O:THF solution (**4**). **$U(N^tBu)_2(SPh)_2(py)_2$ (3-S)**: ^{1}H NMR ($CDCl_3$, 293 K): δ 0.06 (s, 18H, ^{t}Bu), 6.82 (t, 2H, SPh *p*-H), 7.20 (t, 4H, SPh *m*-H), 7.68 (d, 4H, SPh *o*-H), 8.01 (br s, 4H, py *m*-H), 8.21 (br s, 2H, py *p*-H), 10.40 (br s, 4H, py *o*-H) ppm. $^{13}C\{^1H\}$ NMR (THF-d_8, 293 K): δ 34.71, 74.01, 123.50, 126.54, 128.60, 131.21, 135.77, 137.36, 150.16 ppm. Analysis Calc. (C, 47.61; H, 5.06; N, 7.10) Found (C, 43.73; H, 5.02; N, 6.64) **$U(N^tBu)_2(SePh)_2(py)_2$ (3-Se)**: ^{1}H NMR (THF-d_8, 293 K) δ 0.30 (s, 18H, ^{t}Bu), 6.83 (t, 2H, SePh *p*-H), 7.05 (t, 4H, SePh *m*-H), 7.42 (br s, 4H, py *m*-H), 7.78 (br s, 2H, py *p*-H), 8.05 (d, 4H, SePh *o*-H), 8.83 (br s, 4H, py *o*-H) ppm. $^{13}C\{^1H\}$ NMR (THF-d_8, 293 K): δ 34.68, 74.24, 124.23, 126.54, 128.61, 131.11, 135.77, 142.36, 150.12 ppm. Analysis Calc. (C, 42.36; H, 4.50; N, 6.59) Found (C, 36.61; H, 4.23; N, 6.10) **$U(N^tBu)_2(TePh)_2(py)_2$ (3-Te)**: ^{1}H NMR (THF-d_8, 293 K) δ 0.30 (s, 18H, ^{t}Bu), 6.83 (t, 2H, TePh *p*-H), 7.05 (t, 4H, TePh *m*-H), 7.42 (br s, 4H, py *m*-H), 7.78 (br s, 2H, py *p*-H), 8.05 (d, 4H, TePh *o*-H), 8.83 (br s, 4H, py *o*-H) ppm. $^{13}C\{^1H\}$ NMR (THF-d_8, 293 K): δ 33.89, 76.56, 121.71, 125.25, 128.60, 131.21, 142.07, 148.03, 149.30 ppm. Analysis Calc. (C, 38.01; H, 4.04; N, 5.81) Found (C, 33.33; H, 3.86; N, 5.35) **$[Na(thf)_2]_2[U(N^tBu)_2(SPh)_4]$ (4-S)**: ^{1}H NMR (THF-d_8, 293 K): δ 0.12 (s, 18H, ^{t}Bu), 6.65 (br t, 4H, *p*-H), 6.99 (br t, 8H, *m*-H), 8.07 (br s, 8H, *o*-H) ppm. $^{13}C\{^1H\}$ NMR (THF-d_8, 293 K): δ 35.83, 77.14, 122.17, 127.19, 135.51, 150.88 ppm. Analysis Calc. (C, 44.54; H, 4.44; N, 3.25) Found (C, 44.49; H, 4.88; N, 3.37) **$[Na(thf)_2]_2[U(N^tBu)_2(SePh)_4]$ (4-Se)**: ^{1}H NMR (THF-d_8, 293 K): δ 0.21 (s, 18H, ^{t}Bu), 1.85 (br s, 16 H, THF), 3.81 (br s, 16 H, THF), 7.01 (t, 4H, *p*-H), 7.18 (t, 8H, *m*-H), 8.13 (d, 8H, *o*-H) ppm. $^{13}C\{^1H\}$ NMR (THF-d_8, 293 K): δ 35.31, 75.89, 120.98, 130.26, 148.27 ppm. Analysis Calc. (C, 36.59; H, 4.65; N, 3.25) Found (C, 36.80; H, 4.43; N, 3.37) **$[Na(thf)_2]_2[U(N^tBu)_2(TePh)_4]$ (4-Te)**: ^{1}H NMR (THF-d_8, 293 K): δ 0.36 (s, 18H, ^{t}Bu), 6.75 (br t, 4H, *p*-H), 6.88 (br t, 8H, *m*-H), 8.19 (br s, 8H, *o*-H) ppm. $^{13}C\{^1H\}$ NMR (THF-d_8, 293 K): δ 35.01, 75.41, 121.38, 124.63, 142.66 ppm. Analysis Calc. (C, 30.87; H, 3.08; N, 2.25) Found (C, 30.66; H, 3.66; N, 2.59)

$U(NDipp)(NHDipp)_2(^tBu_2bpy)_2$ (5). THF (5 mL) was added to a solid mixture of UCl_4 (200 mg, 0.52 mmol) and $^tBu_2$bpy (284 mg, 1.05 mmol, 2 equiv). Stirring the mixture at room temperature rapidly formed a dark green solution. To this was added LiNHDipp (420 mg, 2.10 mmol, 4 equiv.) as a solid at room temperature. The solution, which had immediately turned dark brown, was stirred overnight, after which time the volatile materials were removed under vacuum to yield an oily brown solid. The material was washed with hexane (2 x 3 mL) then dissolved in toluene (2 mL) and filtered through Celite. Vapor diffusion of hexane into the toluene solution produced black crystals of the product. **$U(NDipp)(NHDipp)_2(^tBu_2bpy)_2$ (5)**: ^{1}H NMR (C_6D_6, 293 K): δ -2.40 (s, 12H, 40 Hz), -2.24 (s, 12H, 40 Hz), -1.03 (s, 2H, 10 Hz), 2.23 (s, 1H, 10 Hz), 3.79 (vbs, 18H, 110 Hz), 5.62 (vbs, 18H, 120 Hz), 9.05 (bs, 4H, 60 Hz), 12.59 (s, 4H, 15 Hz), 18.65 (s, 2H, 15 Hz), 24.69 (s, 4H, 25Hz). Analysis Calc. (C, 66.39; H, 7.82; N, 7.53) Found (C, 63.49; H, 7.84; N, 7.13)

Conclusions

The previously reported observation that a U(IV) complex of uncertain composition was capable of performing halogen atom

abstraction from dihalomethanes to generate U(V) *bis*(imido) species prompted a broader study to understand the nature of the U(IV) intermediate. This species was found to be the seven-coordinate imido/*bis*(amido) complex **5**. Notably, this complex exhibits an extremely long U=NDipp distance of 2.100 Å, the longest uranium imido distance known to date. The identification of this species, coupled with its known reaction chemistry to form U(V) *bis*(imido) complexes, prompted our investigation into whether or not similar U(IV) species could serve as synthons for higher valent *bis*(imido) frameworks. It appears that irrespective of the protonation state of the NR-containing units, oxidation of the U(IV) center prompts alpha-hydrogen abstraction (if necessary) to generate the U(VI) *trans-bis*(imido) motif.

Conflicts of interest

There are no conflicts to declare.

Acknowledgements

The acknowledgements come at the end of an article after the conclusions and before the notes and references.

Notes and references

1. T. W. Hayton, *Dalton Transactions*, 2010, **39**, 1145-1158.
2. T. W. Hayton, *Chemical Communications*, 2013, **49**, 2956-2973.
3. M. B. Jones and A. J. Gaunt, *Chemical Reviews*, 2013, **113**, 1137-1198.
4. L. S. T., *Angewandte Chemie International Edition*, 2015, **54**, 8604-8641.
5. T. Straub, A. Haskel, T. G. Neyroud, M. Kapon, M. Botoshansky and M. S. Eisen, *Organometallics* 2001, **20**, 5017.
6. W. Ren, G. Zi, D.-C. Fang and M. D. Walter, *J. Am. Chem. Soc.*, 2011, **133**, 13183-13196.
7. W. Ren, G. Zi, D.-C. Fang and M. D. Walter, *Chem. Eur. J.*, 2011, **17**, 12669.
8. W. Ren, G. Zi and M. D. Walter, *Organometallics*, 2012, **31**, 672.
9. N. L. Bell, L. Maron and P. L. Arnold, *J. Am. Chem. Soc.*, 2015, **137**, 10492.
10. A. Haskel, T. Straub and M. S. Eisen, *Organometallics* 1996, **15**, 3773.
11. D. M. King, J. McMaster, F. Tuna, E. J. L. McInnes, W. Lewis, A. J. Blake and S. T. Liddle, *J. Am. Chem. Soc.*, 2014, **136**, 5619-5622.
12. R. E. Jilek, N. C. Tomson, R. L. Shook, B. L. Scott and J. M. Boncella, *Inorganic Chemistry*, 2014, **53**, 9818-9826.
13. B. M. Gardner, G. Balazs, M. Scheer, F. Tuna, E. J. L. McInnes, J. McMaster, W. Lewis, A. J. Blake and S. T. Liddle, *Angewandte Chemie-International Edition*, 2014, **53**, 4484-4488.
14. N. H. Anderson, S. O. Odoh, Y. Yao, U. J. Williams, B. A. Schaefer, J. J. Kiernicki, A. J. Lewis, M. D. Goshert, P. E. Fanwick, E. J. Schelter, J. R. Walensky, L. Gagliardi and S. C. Bart, *Nature Chemistry*, 2014, **6**, 919-926.
15. D. M. King, F. Tuna, E. J. L. McInnes, J. McMaster, W. Lewis, A. J. Blake and S. T. Liddle, *Nature Chemistry*, 2013, **5**, 482-488.
16. O. P. Lam, S. M. Franke, H. Nakai, F. W. Heinemann, W. Hieringer and K. Meyer, *Inorganic Chemistry*, 2012, **51**, 6190-6199.
17. D. M. King, F. Tuna, E. J. L. McInnes, J. McMaster, W. Lewis, A. J. Blake and S. T. Liddle, *Science*, 2012, **337**, 717-720.
18. R. E. Jilek, L. P. Spencer, R. A. Lewis, B. L. Scott, T. W. Hayton and J. M. Boncella, *J. Am. Chem. Soc.*, 2012, **134**, 9876-9878.
19. R. E. Jilek, L. P. Spencer, D. L. Kuiper, B. L. Scott, U. J. Williams, J. M. Kikkawa and J. M. Boncella, *Inorg. Chem.*, 2011, **50**, 4235-4237.
20. L. P. Spencer, P. Yang, B. L. Scott, E. R. Batista and J. M. Boncella, *Inorganic Chemistry*, 2009, **48**, 2693-2700.
21. T. W. Hayton and G. Wu, *J. Am. Chem. Soc.*, 2008, **130**, 2005.
22. C. R. Graves, P. Yang, S. A. Kozimor, A. E. Vaughn, D. L. Clark, S. D. Conradson, E. J. Schelter, B. L. Scott, J. D. Thompson, P. J. Hay, D. E. Morris and J. L. Kiplinger, *J. Am. Chem. Soc.*, 2008, **130**, 5272-5285.
23. C. R. Graves, A. E. Vaughn, E. J. Schelter, B. L. Scott, J. D. Thompson, D. E. Morris and J. L. Kiplinger, *Inorganic Chemistry*, 2008, **47**, 11879-11891.
24. P. L. Arnold, D. Patel, C. Wilson and J. B. Love, *Nature*, 2008, **451**, 315.
25. C. R. Graves, B. L. Scott, D. E. Morris and J. L. Kiplinger, *J. Am. Chem. Soc.*, 2007, **129**, 11914-+.
26. T. W. Hayton, J. M. Boncella, B. L. Scott, E. R. Batista and P. J. Hay, *J. Am. Chem. Soc.*, 2006, **128**, 10549-10559.
27. T. W. Hayton, J. M. Boncella, B. L. Scott and E. R. Batista, *J. Am. Chem. Soc.*, 2006, **128**, 12622-12623.
28. I. Castro-Rodriguez, H. Nakai and K. Meyer, *Angewandte Chemie-International Edition*, 2006, **45**, 2389-2392.
29. T. W. Hayton, J. M. Boncella, B. L. Scott, P. D. Palmer, E. R. Batista and P. J. Hay, *Science*, 2005, **310**, 1941-1943.
30. J.-C. Berthet, M. Nielich and M. Ephritikhine, *Angew. Chem. Int. Ed.*, 2003, **42**, 1952.
31. P. B. Duval, C. J. Burns, W. E. Buschmann, D. L. Clark, D. E. Morris and B. L. Scott, *Inorganic Chemistry*, 2001, **40**, 5491-5496.
32. D. S. J. Arney, R. C. Schnabel, B. C. Scott and C. J. Burns, *J. Am. Chem. Soc.*, 1996, **118**, 6780-6781.
33. D. S. J. Arney and C. J. Burns, *J. Am. Chem. Soc.*, 1995, **117**, 9448-9460.
34. D. S. J. Arney and C. J. Burns, *J. Am. Chem. Soc.*, 1993, **115**, 9840-9841.
35. D. S. J. Arney, C. J. Burns and D. C. Smith, *J. Am. Chem. Soc.*, 1992, **114**, 10068-10069.
36. H. Anderson Nickolas, H. Yin, J. Kiernicki John, E. Fanwick Phillip, J. Schelter Eric and C. Bart Suzanne, *Angewandte Chemie International Edition*, 2015, **54**, 9386-9389.
37. N. H. Anderson, J. Xie, D. Ray, M. Zeller, L. Gagliardi and S. C. Bart, *Nature Chemistry*, 2017, **9**, 850.
38. J. L. Brown, S. Fortier, G. Wu, N. Kaltsoyannis and T. W. Hayton, *Journal of the American Chemical Society*, 2013, **135**, 5352-5355.

39. J. L. Brown, S. Fortier, R. A. Lewis, G. Wu and T. W. Hayton, *Journal of the American Chemical Society*, 2012, **134**, 15468-15475.
40. J. L. Brown, E. R. Batista, J. M. Boncella, A. J. Gaunt, S. D. Reilly, B. L. Scott and N. C. Tomson, *J. Am. Chem. Soc.*, 2015, **137**, 9583-9586.
41. M. L. Neidig, D. L. Clark and R. L. Martin, *Coordination Chemistry Reviews*, 2013, **257**, 394.
42. N. H. Anderson, Ph.D., Purdue University, 2016.
43. W. J. Evans, M. K. Takase, J. W. Ziller, A. G. DiPasquale and R. L. Rheingold, *Organometallics*, 2009, **28**, 236.
44. S. M. Franke, M. W. Rosenzweig, F. W. Heinemann and K. Meyer, *Chemical Science*, 2015, **6**, 275-282.
45. R. D. Shannon, *Acta Cryst.* , 1976, **A32**, 751.
46. E. M. Matson, A. T. Breshears, J. J. Kiernicki, B. S. Newell, P. E. Fanwick, M. P. Shores, J. R. Walensky and S. C. Bart, *Inorg. Chem.*, 2014, **53**, 12977.
47. R. G. Peters, B. P. Warner, B. L. Scott and C. J. Burns, *Organometallics*, 1999, **18**, 2587.
48. S. Fortier, J. Veleta, A. Pialat, J. Le Roy, K. B. Ghiassi, M. M. Olmstead, A. Metta-Magaña, M. Murugesu and D. Villagrán, *Chemistry – A European Journal*, 2016, **22**, 1931-1936.
49. V. Iluc and G. L. Hillhouse, *J. Am. Chem. Soc.*, 2010, **132**, 15148.
50. R. E. Cowley, R. P. Bontchev, J. Sorrell, O. Sarracino, Y. Feng, H. Wang and J. M. Smith, *J. Am. Chem. Soc.*, 2007, **129**, 2424.
51. M. G. Schelbel, J. Abbenseth, M. Kinauer, F. W. Heinemann, C. Würtele, B. de Bruin and S. Schneider, *Inorg. Chem.*, 2015, **54**, 9290.
52. M. H. V. Hyunh and T. J. Meyer, *Proc. Nat. Acad. Sci.*, 2004, **101**, 13138.
53. J. L. Kiplinger, D. E. Morris, B. L. Scott and C. J. Burns, *Organometallics*, 2002, **21**, 5978.
54. N. A. Eckert, J. M. Smith, R. M. Lachicotte and P. L. Holland, *Inorg. Chem.*, 2004, **43**, 3306.